Def Sci J, Vol 32, No 4, October 1982, pp 339-345

Hydromagnetic Unsteady Flow of a Dusty Viscous Fluid Between a Flat Wall and a Long Wavy Wall

P. SAKUNTHALA & D. BATHAIAH

Department of Mathematics, Sri Venkateswara University College, Tirupati-517 502

Received 11 August 1981; revised 28 January 1982

Abstract. Magnetohydrodynamic flow of a dusty viscous conducting fluid between a parallel flat wall and a long wavy wall has been studied The velocity distributions of fluid and dust and the coefficients of skin-friction at both the walls have been evaluated. The effects of magnetic and frequency parameters on the above said physical quantities have been investigated.

1. Introduction

The interest in the study of transport of solid particles by fluids, which has been engaging the attention of several scientists and engineers for a long time, has been enhanced by the recent use of high-energy solid rocket propellants. This topic finds applications in such diverse fields as the transportation of sediment by water and air, the centrifugal separation of particulate matter from fluids, fluid-droplet sprays, fluidised beds and other two-phase flow phenomena of interest in chemical processing, the electro static precipitation of dust, blood flow and so on. There are many situations involving the motion of dusty viscous fluids in the presence of magnetic field. For instance, the flow of a dusty viscous fluid on any celestial body occurs under the influenced magnetic field of the body. The flow of dust-laden air takes place under the influence of the earth's magnetic field. Thus it is interesting to study the effect of the magnetic field on the motion of the dusty viscous fluids.

Viscous fluid flow over a wavy wall has attracted the attention of relatively few researchers although the analysis of such flows finds application in such different areas as transpiration cooling of re-entry vehicles and rocket boosters, cross hatching on ablative surfaces and film vapourization in cumbustion chambers. Shankar & Sinha[1] have made a detailed study of the Rayleigh problem for a wavy wall. They have concluded that at low Reynolds numbers the wavyness of the wall quickly ceases to be of importance as the liquid is dragged along by the wall, where at large Reynolds numbers the effects of viscosity are confined to a thin layer close to the wall and known potential solution emerges in time. Vajravelu & Sastry[2] have devoted attention to the effect of wavyness of one of the walls on the flow and heat transfer characteristics of an incompressible viscous fluid confined between two long vertical walls and set in motion

by a difference in the wall temperatures. Lekoudis, Neyfeh & Saric[3] have studied the compressible boundary layer flows over a wavy wall. Lessen & Gangwani[4] have investigated the effects of small amplitude wall wavyness upon the stability of the laminar boundary layer. Interest in problems of mechanics of system with more than one phase has developed rapidly in recent years. Work in this field has been carried out by Saffman[5], Michael[6], Rao[7] and Verma & Mathur[8]. In this paper we study the magnetohydrodynamic flow of a dusty viscous conducting fluid between a parallel flat wall and a long wavy wall. The flow configuration is shown in Fig. A. X-axis is taken along the parallel flat wall and a straight line perpendicular to that as the Y-axis, so that the wavy wall is represented by $y = \epsilon^* \cos \lambda^* x$ and the flat wall by $y = 0$. We assume that the wave length of the wavy wall which is proportional to $\frac{1}{K}$ is large. Taking the fluid to be of small conductivity with magnetic Reynolds number much less than unity, the induced magnetic field is neglected in comparison with the applied magnetic field[9].

2. Formulation and Solution of the Problem

In the absence of any input electric field the equations governing the fluid flow, containing solid particles[5] are

$$\frac{\partial \bar{u}}{\partial t} + (\bar{u} \cdot \nabla)\,\bar{u} = -\frac{1}{\rho}\nabla P + \nu \nabla^2 \bar{u} + \frac{KN}{\rho}(\bar{v} - \bar{u}) + \frac{\mu_e}{\rho}(\bar{J} \times \bar{H}) \quad (1)$$

$$m\left(\frac{\partial \bar{v}}{\partial t} + (\bar{v} \cdot \nabla)\,\bar{v}\right) = K(\bar{u} - \bar{v}) \quad (2)$$

$$\nabla \cdot \bar{u} = 0 \quad (3)$$

$$\frac{\partial \bar{N}}{\partial t} + \operatorname{div}(N\bar{v}) = 0 \quad (4)$$

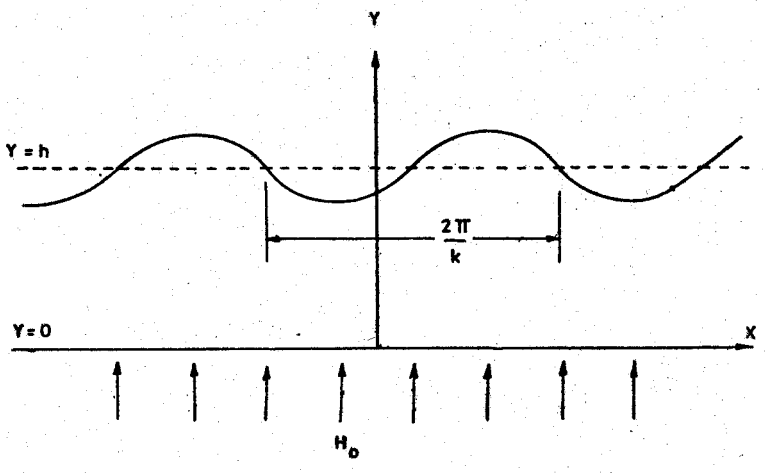

Figure A. Flow Configuration.

where

$\bar{u} = (u_1, 0, 0)$ is the velocity of the fluid particles

$\bar{v} = (v_1, 0, 0)$ is the velocity of the solid particles

ρ the fluid density, P the fluid pressure, ν the kinematic coefficient of viscosity of the fluid, K the resistance coefficient of dust particles, N the number density of the dust particles, m the mass of each dust particles, t the time, $\bar{J}$ the current density and $\bar{H} = (0, H_o, 0)$ the magnetic field.

The boundary conditions are

$$u_1 = 0, v_1 = 0 \quad \text{at } y = 0 \tag{5a}$$

$$u_1 = 0, v_1 = 0 \quad \text{at } y = \epsilon^* \cos \lambda^* x \tag{5b}$$

We define the following dimensionless parameters

$$x^1 = \frac{x}{h}, y^1 = \frac{y}{h}, u = \frac{u_1 h}{\nu}, v = \frac{v_1 h}{\nu}$$

$$P^1 = \frac{Ph^2}{\rho \nu^2}, t^1 = \frac{\nu t}{h^2}, l = \frac{mN}{\rho}, a = \frac{m\nu}{Kh^2} \tag{6}$$

In view of Eqn. (6), Eqns. (1) and (2) reduce to (dropping the primes)

$$\frac{\partial u}{\partial t} = -\frac{\partial P}{\partial x} + \frac{\partial^2 u}{\partial y^2} + \frac{l}{a}(v - u) - Mu \tag{7}$$

$$\frac{\partial v}{\partial t} = \frac{l}{a}(u - v) \tag{8}$$

where $M = \dfrac{\sigma \mu_e^2 H_0^2 h^2}{\mu}$ (Magnetic parameter)

From Eqns. (7) and (8), we obtain

$$\frac{\partial^2 u}{\partial t^2} + \left(\frac{1}{a} + \frac{l}{a} + M\right)\frac{\partial u}{\partial t} = \frac{c}{a} + \frac{1}{a}\frac{\partial^2 u}{\partial y^2} + \frac{\partial^3 u}{\partial t \partial y^2} - \frac{Mu}{a} \tag{9}$$

where $c = -\dfrac{\partial P}{\partial x} = \text{constant}$

The boundary conditions in the non-dimensional form are

$$u = 0, v = 0 \text{ at } y = 0$$

$$u = 0, v = 0 \text{ at } y = \epsilon \cos \lambda x \tag{10}$$

where

$\epsilon = \dfrac{\epsilon^*}{h}$ (non-dimensional amplitude parameter).

$\lambda = \lambda^* h$ (non-dimensional frequency parameter).

We define Laplace Transform as

$$\bar{u} = \int_0^\infty e^{-st}\, u dt \tag{11}$$

with the inversion

$$u = \frac{1}{2\pi i} \int_{r-i\infty}^{r+i\infty} \bar{u} e^{st}\, ds \tag{12}$$

Using Eqn. (11), Eqn. (9) transforms into

$$\frac{\partial^2 \bar{u}}{\partial y^2} - b^2 \bar{u} = \frac{-c}{s(1+sa)} \tag{13}$$

where $$b^2 = \frac{as^2 + s + ls + aMs + M}{1 + sa}$$

The boundary conditions are

$$\bar{u} = 0 \quad \text{at } y = 0$$

$$\bar{u} = 0 \quad \text{at } y = \epsilon \cos \lambda x \tag{14}$$

Using Eqn. (14), solving Eqn. (13), we obtain

$$\bar{u} = \frac{c}{b^2 s(1+sa)} \left[1 + \frac{\sinh\{b(y - \epsilon \cos \lambda x)\}}{\sinh(b\epsilon \cos \lambda x)} - \frac{\sinh by}{\sinh(b\epsilon \cos \lambda x)}\right] \tag{15}$$

Inverting the Eqn. (15) by using Eqn. (12), we get

$$u = Q_1 \sin q(y - \epsilon \cos \lambda x) + Q_2 \sin q\,(y - \epsilon \cos \lambda x)$$

$$- Q_1 \sin qy - Q_2 \sin qy + \frac{c}{M} \frac{\sin h \sqrt{M}(y - \epsilon \cos \lambda x)}{\sinh \sqrt{M} \epsilon \cos \lambda x}$$

$$- \frac{c}{M} \frac{\sinh \sqrt{M} y}{\sinh \sqrt{M} \epsilon \cos \lambda x} + \frac{c}{M} \tag{16}$$

Using Eqns. (7) and (16), we get

$$v = \frac{a}{l} [- \alpha_1 Q_1 \sin q(y - \epsilon \cos \lambda x) - \alpha_2 Q_2 \sin q(y - \epsilon \cos \lambda x)$$

$$+ \alpha_1 Q_1 \sin qy + \alpha_2 Q_2 \sin qy] - \frac{ac}{l} - \frac{a}{l}$$

$$\times \left[- c \frac{\sinh \sqrt{M} y}{\sinh \sqrt{M}\, \epsilon \cos \lambda x} + c \frac{\sinh \sqrt{M}(y - \epsilon \cos \lambda x)}{\sinh \sqrt{M}\, \epsilon \cos \lambda x} \right.$$

$$\left. + q^2 Q_1 \sin q(y - \epsilon \cos \lambda x) - q^2 Q_2 \sin q(y - \epsilon \cos \lambda x) - q^2 Q_1 \sin qy \right.$$

$$+ q^2 Q_2 \sin qy \Big] + \left(1 + \frac{Ma}{l}\right) \Big[\frac{c}{M} + \frac{c}{M} \frac{\sinh \sqrt{M}(y - \epsilon \cos \lambda x)}{\sinh \sqrt{M} \epsilon \cos \lambda x}$$

$$- \frac{c}{M} \frac{\sinh \sqrt{M} y}{\sinh \sqrt{M} \epsilon \cos \lambda x} + Q_1 \sin q\,(y - \epsilon \cos \lambda x)$$

$$+ Q_2 \sin q(y - \epsilon \cos \lambda x) - Q_1 \sin qy - Q_2 \sin qy \Big]$$

where

$$Q_1 = \frac{- \sum_{n=1}^{\infty} (-1)^n 2c(1 + \alpha_1 a)^2 e^{\alpha_1 t} n\pi}{\epsilon^2 \cos^2 \lambda x [(1 + \alpha_1 a)\{2\alpha_1 - (\beta_1 + \beta_2)\} - (\alpha_1 - \beta_1)(\alpha_1 - \beta_2) a] \times \alpha_1(\alpha_1 - \beta_1)(\alpha_1 - \beta_2)}$$

$$Q_2 = \frac{- \sum_{n=1}^{\infty} (-1)^n 2c(1 + \alpha_2 a)^2 e^{\alpha_2 t} n\pi}{\epsilon^2 \cos^2 \lambda x [(1 + \alpha_2 a)\{2\alpha_2 - (\beta_1 + \beta_2)\} - (\alpha_2 - \beta_1)(\alpha_2 - \beta_2) a] \times \alpha_2(\alpha_2 - \beta_1)(\alpha_2 - \beta_2)}$$

$$q = \frac{n\pi}{\epsilon \cos \lambda x}$$

$$\alpha_1 = \frac{(r_1^2 - 4r_2)^{1/2} + r_1}{2}$$

$$\alpha_2 = -\left[\frac{(r_1^2 - 4r_2)^{1/2} - r_1}{2}\right]$$

$$r_1 = \beta_1 + \beta_2 - \frac{an^2\pi^2}{\epsilon^2 \cos^2 \lambda x}$$

$$r_2 = \beta_1 \beta_2 + \frac{an^2\pi^2}{\epsilon^2 \cos^2 \lambda x}$$

$$\beta_1 = \frac{(\alpha^2 - 4aM)^{1/2} - \alpha}{2}$$

$$\beta_2 = -\left[\frac{(\alpha^2 - 4aM)^{1/2} + \alpha}{2}\right]$$

$$\alpha = 1 + l + aM$$

3. Skin Friction

The skin friction at the lower plate $y = 0$ is

$$C_f = \mu \left(\frac{\partial u}{\partial y}\right)_{y=0}$$

$$= \mu\left[(Q_1 + Q_2)\{(-1)^n - 1\} - \frac{c}{\sqrt{M}}\,\text{cosech}\,\sqrt{M}\epsilon\cos\lambda x \times \{\cosh\sqrt{M}\epsilon\cos\lambda x - 1\}\right]$$

The skin friction at the wavy plate $y = \epsilon\cos\lambda x$ is

$$C_f^* = -C_f.$$

4. Conclusions

We have investigated the effects of magnetic and frequency parameters on the fluid and dust velocities and also on the skin friction. In Fig. 1, we have plotted the graph $-u$ against y for different values of magnetic parameter M. We have observed that

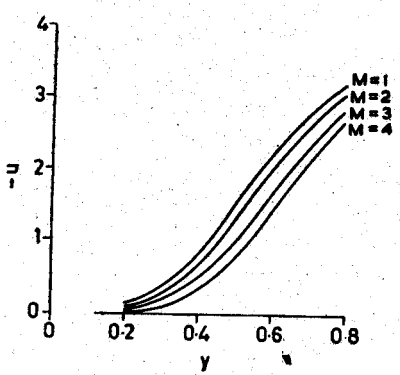

Figure 1. Fluid velocity against y for different values of M.

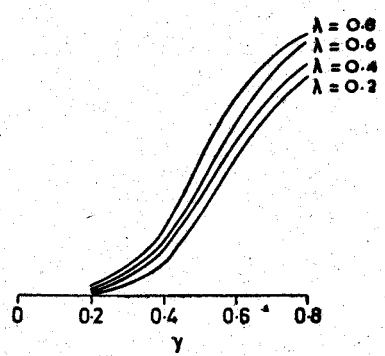

Figure 2. Fluid velocity against y for different values of λ.

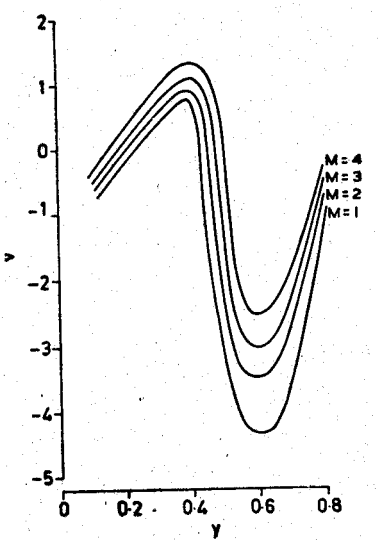

Figure 3. Dust velocity against y for different values of M.

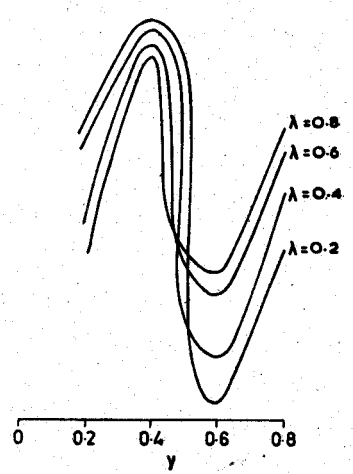

Figure 4. Dust velocity against y for different values of λ.

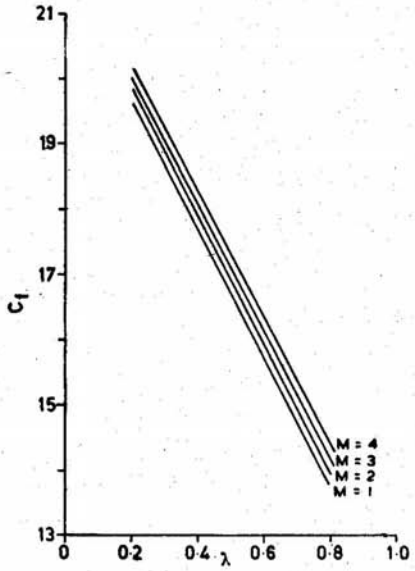

Figure 5. Skin friction against λ for different values of M.

the fluid velocity u increases as M increases. In Fig. 2, we have drawn a graph $-u$ against y for different values of λ. We have seen that the fluid velocity decreases with the increase in λ. The effects of magnetic parameter M and frequency parameter λ are shown in Figs. 3 and 4 respectively.

In Fig. 5, the skin friction C_f is plotted against λ for different values of M. It is observed that the skin friction at the lower plate increases as the magnetic parameter M increases whereas the skin friction at the wavy plate decreases as M increases. It is also seen that the skin friction at the lower plate decreases with the increase in frequency parameter λ whereas the skin friction increases with the increase in λ at the wavy plate.

References

1. Shankar, P. N. & Sinha, V. N., *J. Fluid Mech.*, **77** (1976), 243.
2. Vajravelu, K. & Sastry, K. S., *J. Fluid Mech.*, **86** (1978), 365.
3. Lekoudis, S. G., Neyfeh, A. H. & Saric, W. S., *Phys. Fluids*, **19** (1976), 514.
4. Lessen, M. & Gangwani, S. T., *Phys. Fluids*, **19** (1976), 510.
5. Saffman, P. G., *J. Fluid Mech.*, **13** (1962), 120–128.
6. Michael, D. H., *J. Fluid Mech.*, **31** (1968), 175.
7. Rao, P., *Def. Sci. J.*, **19** (1969), 135.
8. Verma, P. D. & Mathur, A. K., *Ind. J. Pure and Appl. Math.*, **4** (1973), 133.
9. Sparrow, E. M. & Cess, R. D., *Trans. ASME, J. Appl. Mech.*, **29** (1962), 181.